CLOSED–SHELL PSEUDO–ATOMS

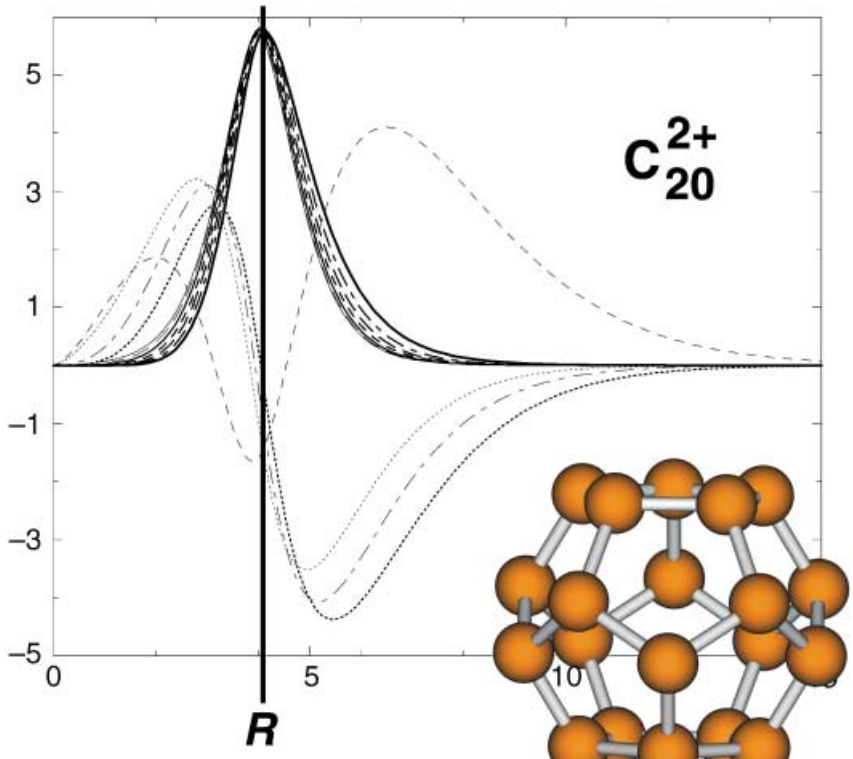

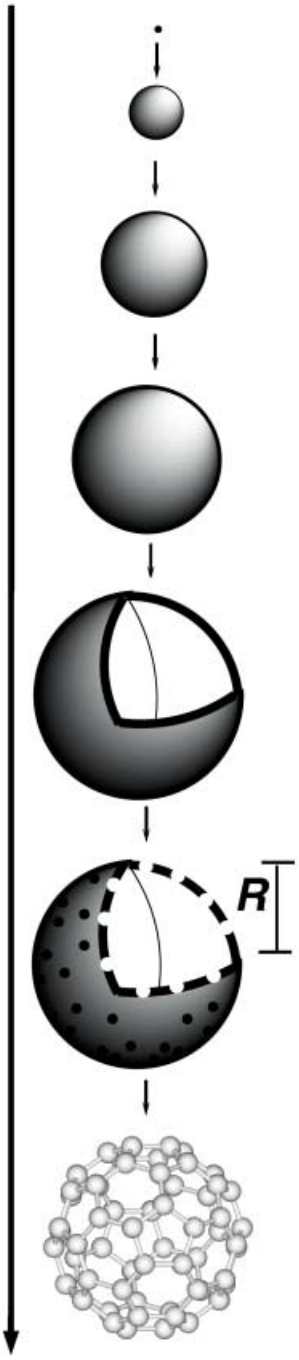

$2(N+1)^2$ rule

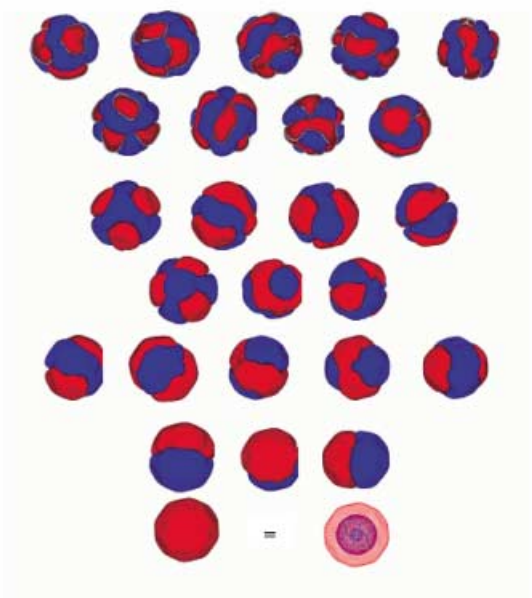

SPHERICAL AROMATICITY

DOI: 10.1002/chem.200304812 *Chem. Eur. J.* **2003**, *9*, 5442 – 5452

From Rare Gas Atoms to Fullerenes: Spherical Aromaticity Studied From the Point of View of Atomic Structure Theory

Markus Reiher*[a] and Andreas Hirsch*[b]

Abstract: The characteristic features of molecules like polyhedra and fullerenes, which follow the $2(N+1)^2$ rule of spherical aromaticity, can be related to energetically stable closed-shell configurations of (pseudo-)atoms. This unifying view relies on a thought experiment, which produces a polyhedron in a two-step process and which can, in turn, relate the electronic configuration of any spherical polyhedron to the one of a corresponding closed-shell atom. In the first step, the electronic ground-state configuration is identified. In the second step, a group theoretical analysis can be carried out; this relates the spherically symmetric atomic orbitals to the molecular orbitals classified according to the irreducible representations of the point group of the polyhedron under consideration. This procedure explains and justifies the pseudo-*l* classification of molecular orbitals, which is the basis of the $2(N+1)^2$ rule. For the transition from the electronic configuration of the rare gas Eka-Rn (Uuo) to the icosahedral fullerene C_{20}^{2+}, we show how a change in the ground-state configuration leads to the phenomenologically found $2(N+1)^2$ rule for spherically aromatic fullerenes.

Keywords: ab initio calculations · aromaticity · atomic structure theory · fullerenes

Introduction

A phenomenological observation on several I_h-symmetric fullerenes revealed similarities of the fullerene's molecular orbitals with radial-symmetric atomic orbitals.[1] Consequently, a pseudo-*l* classification of these valence molecular orbitals was possible. Such a classification scheme was also found by Martins, Troullier, and Weaver for C_{60}. It was used as a means for a qualitative understanding of one-electron states in buckminsterfullerene.[2] However, the possibility of interrelating spherical molecules on the basis of such a scheme and of identifying molecules with contiguously filled pseudo-*l* shells as "aromatic" was only recognized in:[1] Along with the *l* classification came the observation that the *l*-classified molecular orbitals show a sequence of monotonously increasing *l* value with decreasing absolute value of the orbital energy,[1] that is, the highest occupied orbital can be classified by a pseudo-angular quantum number $l_{\mathrm{HOMO}} = l_{\max}$, then the next lowest orbital has $l_{\mathrm{HOMO}-1} = l_{\max} - 1$, the following has $l_{\mathrm{HOMO}-2} = l_{\max} - 2$, and so on until we finally find an s-like shell $l_{\mathrm{HOMO}-n} = 0$. Counting electrons in these completely filled pseudo-*l* states led to the $2(N+1)^2$ rule (in which N equals $l_{\max}$), which states that spherical systems with $2(N+1)^2$ π-electrons exhibit spherical aromaticity.[1]

The most important aspect of the $2(N+1)^2$ rule is that it postulates a certain ordering of pseudo-*l*-classified molecular orbitals and a Hückel-like (i.e., Hückel aromatic) stability for spherical systems without reference to a particular class of molecules. Three-dimensional aromaticity (see, e.g., refs. [3, 4]) has attracted considerable attention, and several concepts and rules for their description have been suggested. For example, Deza et al. used graph theoretical approaches in order to recover concepts of Hückel theory for structurally different fullerenes.[5] King has investigated three-dimensional aromaticity in boranes by using models that originated from nuclear physics.[6, 7] King also described the pseudo-*l* classification of molecular orbitals of C_{60} in spherical symmetry.[8, 9] He used capital letters for the classification S, P, D, F, G, … of the shells. However, since the shells represent one-electron states we stick in this work to the common use of small letters s, p, d, f, g, … for one-electron states. Miller and Verkade rediscovered the shell structure of molecular orbitals in fullerenes and analyzed the orbitals in terms of a spherical and of a Hückel-type electronic structure model.[10] Fowler and collaborators qualitatively discussed possible pseudo-*l* orderings in fullerenes from the point of view of graph theory and group theory.[11] They suggested to study these orderings in a quantitative spherical model. Such a type of model was proposed by Stone.[12, 13] Another example is the so-called

[a] Priv. Doz. Dr. M. Reiher
Theoretische Chemie, Universität Erlangen-Nürnberg
Egerlandstrasse 3, 91058 Erlangen (Germany)
Fax: (+49)-9131-85-27736
E-mail: markus.reiher@chemie.uni-erlangen.de

[b] Prof. Dr. A. Hirsch
Institut für Organische Chemie
Universität Erlangen-Nürnberg, Henkestrasse 42
91054 Erlangen (Germany)
Fax: (+49)9131-85-26864
E-mail: hirsch@chemie.uni-erlangen.de

 DOI: 10.1002/chem.200304812

"jellium" model in physics for the description of clusters (see next section for details). In this work, we also exploit the spherical symmetry in order to solve radial many-particle equations and to model the electronic wave function.

The $2(N+1)^2$ rule has been investigated in detail for several fullerenes and heterofullerenes in terms of magnetic properties of these systems,[14, 15, 16] and the spherical aromaticity concept applied to fullerenes has recently been reviewed in reference [17]. It has also been suggested to extend the spherical electron-counting concept to σ-bonded systems like clusters of hydrogen atoms.[14] Furthermore, it was extended to inorganic cage molecules of Groups 14 and 15 of the periodic table (e.g., the P_4 tetrahedron).[18] Also homoaromaticity has been analyzed in terms of the new electron-counting rule for spherical molecules with cubane, dodecahedrane, and adamantane frameworks.[19] All these studies rely mainly on magnetic criteria for the determination of aromaticity. However, it has often been stated that aromaticity is not a one-dimensional concept[20, 21, 22, 23] and that other criteria like energetical stability should also be taken into account. This multidimensional character of aromaticity has further been analyzed and confirmed by Neus and Schwarz in one of the valuable accounts on the scientific value of the aromaticity concept.[24]

It is interesting to note that some sort of "extended aromaticity" has very recently been found for a $C_{48}N_{12}$ azafullerene.[25] This "extended aromaticity" was dicussed by the authors of reference [25] in terms of the limited *planar* Hückel-type aromaticity and led to a somewhat clumsy description of the aromatic character of this azafullerene. The $2(N+1)^2$ rule provides a more direct description of $C_{48}N_{12}$, which is isoelectronic to C_{60}^{12-}. The electronic configuration of C_{60}^{12-} fulfills the $2(N+1)^2$ rule for $N=5$. Therefore, also the configuration of $C_{48}N_{12}$ represents an example for which a magic electron number of the $2(N+1)^2$ rule is met—in this case by introducing excess electrons through nitrogen–carbon exchange in order to add as many π-electrons to the original C_{60} system as are missing for a stable spherically aromatic electronic configuration.

These findings for several fullerenes are very remarkable, since one would expect to have a rather unpredictable sequence of frontier orbital energies in case of atomic states with more than say 100 electrons, which makes this special, phenomenologically found orbital ordering for pseudo-*l*-classified states of fullerenes appear unlikely. To understand these observations in greater detail, we explicitly take a viewpoint from atomic structure theory and approach the molecular states from atomic structure calculations. We thus aim at an understanding of spherical aromaticity in fullerenes and polyhedra in terms of energetical stability concepts for atoms. Among atoms the rare gas atoms are particularly stable and inert. This fact can, of course, be traced back to their closed-shell electronic structure. It is therefore desirable to investigate whether similar stability criteria can be identified for those fullerenes, which are termed *spherically aromatic* according to the $2(N+1)^2$ rule. For this purpose we construct a transformation which produces a spherical polyhedron from an atom in order to reconstruct the remarkable phenomenological observation of the orbital ordering found for spherically aromatic molecules. Our procedure relates spherical aromaticity of polyhedra to ground-state configurations of closed-shell (pseudo-)atoms. This theoretical approach provides thus a unified view on the *(absolute) energetical* stability of rare gas atoms and aromatic spherical polyhedra.

This work is organized as follows: In the next section we describe the two-step thought experiment that transforms a pseudo-atom into a spherical polyhedron. Afterwards, the electronic structure of C_{20}^{2+} is discussed in terms of our transformation model. We conclude with some general comments on the range of validity of the $2(N+1)^2$ rule and a perspective for future work.

The "Pseudo-Atom" Model of Spherical Clusters and Fullerenes

To establish the rigorous connection between closed-shell atoms, like rare gases and spherical polyhedra, the basis of our theoretical approach is the following thought experiment, which is depicted in Figure 1: We start with a spherically symmetric atom possessing a point-like nucleus. Note that a point-like and a small finite nucleus have almost the same effect on the electronic structure of a (non-relativistic) atom, that is, they can hardly be distinguished in terms of the total electronic energy (see, for instance, reference [26]). In phase I of our experiment, this nuclear charge distribution is expanded and distributed over the thin crust of the resulting hollow

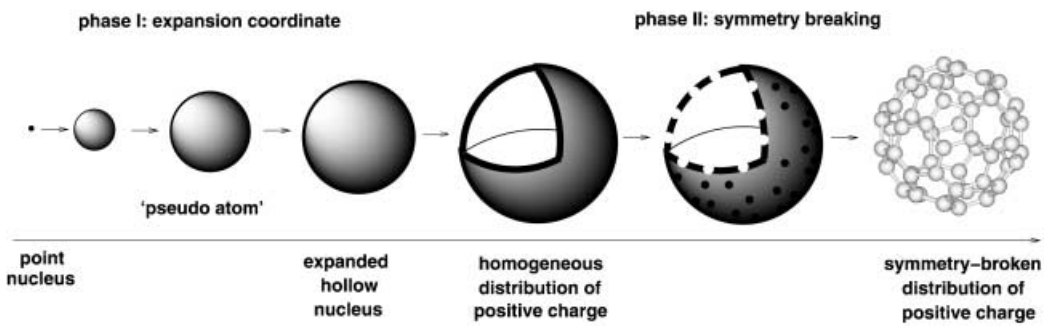

Figure 1. Sketch of the thought experiment for the transformation of a stable, closed-shell atom to an extended cluster with the same number of electrons and protons. In phase I, the point-like nucleus is expanded and the positive charge is homogeneously distributed on the resulting thin sphere. In phase II, this homogeneously distributed charge is contracted to the atomic nuclei positions of the cluster or fullerene to be analyzed.

sphere. Phase II involves a subsequent radial-symmetry breaking by condensation of nuclear charge: the uniformly charged sphere modeling the protons is modified in such a way that positive charge is concentrated at those positions on the sphere where the nucleus positions of the atoms of the spherical polyhedron are.

Phase I of this methodology has some similarities with the so-called jellium model in metal cluster physics (see, for instance, references [27] (p. 142) and [28] (p. 8)). Indeed, the jellium model has also been applied to studies on (charged) buckminsterfullerene. This model describes a valence-only, effective-pseudo-potential atom, in which the nuclear and core-electron charges are modeled by a homogeneously distributed surrogate charge. This physical model is usually applied within a density functional framework. The main conceptual difference of the jellium model when compared with the present work is the neglect of an explicit treatment of the core electrons and the homogeneously distributed surrogate charge. In general, the jellium concept is appropriate, if *non-hollow* metal clusters are to be described, for which the homogeneous positive background charge distribution is a suitable assumption. As already mentioned in the Introduction, the most detailed jellium-type study of a fullerene has been performed by Martins, Troullier, and Weaver on C_{60}.[2] Our methodology deviates from their work in the following points: 1) We do not work within a density functional framework and are, in principle, able to use multi-configuration techniques for cases of different, close-lying electronic configurations and for the study of open-shell systems. 2) We also include the core electrons in our study so that we can model the positive nuclear charges by an infinitely thin sphere at a given radius instead of using one of finite width, which models core electrons and protons by an effective charge acting on the valence electrons.

Yannouleas and Landman studied various charged buckminsterfullerene molecules $C_{60}^{x\pm}$ within an elaborated jellium model, which explicitly treats all $240 \pm x$ valence electrons and which considers the icosahedral symmetry through a crystal-field type approach.[29] Their study aims at an understanding of the physics of charging buckminsterfullerene as a prototype of a mesoscopic sphere with a certain classical capacitance. The ordering of orbital energies, which should meet the requirement of the $2(N+1)^2$ rule, that is, the sequence of valence shells with monotonously increasing l value, has not been investigated in great detail, though this ordering of π-orbitals is visible in the orbital energy spectrum. However, the valence-shell jellium approach should be considered with care, because partially filled shells may introduce severe problems. To avoid partial shell filling, the number of electrons has been adjusted accordingly (i.e., set equal to 250) in reference [30]. This led to a HOMO with $l_{\max} = 4$ though the correct value for the pseudo-l quantum number would be $l_{\max} = 5$. It is therefore advisable to leave the valence-only jellium model and treat *all* electrons in an ab initio framework.

Mingos and Lin extended the jellium model for the study of alkali metal clusters by incorporating crystal-field effects.[31] This study is of value for a detailed investigation of the transferability of the spherical aromaticity concept to inorganic cage molecules,[18] since Mingos and Lin also considered small, "hollow" clusters.

In general, the jellium-model studies do not intend to establish relations between different hollow cluster structures in order to uncover stability rules like those suggested for the class of aromatic systems. Therefore, a more detailed discussion and comparison with jellium-type models appears to be unnecessary for our purposes here, because it does not yield direct contributions to the aromaticity discussion. Instead, we refer to the results by Martins et al. in reference [2] when we encounter similar findings within our study in order to make this work more compact.

Another approach based on atomic-structure theory for the study of clusters is Stone's *tensor surface harmonic model*,[12, 13] which was applied to boranes and transition metal clusters.[32, 33] Also fullerene chemistry has benefited from the cluster studies of Stone and collaborators (see reference [34] and references therein). Stone's approach constructs the molecular wave function within spherical symmetry and can thus account for an l classification of the molecular orbitals. In this respect it can be understood as a particular way of constructing the molecular orbitals. The model has not been used to cover a "dynamical" process, which is described in our formulation in order to understand the emergence of characteristic pseudo-l classified molecular orbitals.

Phase I: Since the spherical symmetry of the atom is not broken in phase I, we use the anzatz given in Equation (1) for the orbitals $\psi_{nlm_l}(\mathbf{r})$ in the total electronic wave function Ψ:[37]

$$\psi_{nlm_l}(\mathbf{r}) = \psi_{nlm_l}(r,\theta,\phi) = \frac{P_{nl}(r)}{r} Y_{lm_l}(\theta,\phi) \tag{1}$$

in which the radial and angular variables are separated (the spin variables are integrated out from the very beginning, since only closed-shell systems are studied here). With this standard formulation, which is well-known from the wave function of the (non-relativistic and field-free) hydrogen atom, the angular variables θ and ϕ can be treated analytically using the spherical harmonics $Y_{lm_l}(\theta,\phi)$, while the radial functions $P_{nl}(r)$ are calculated numerically on a mesh of grid points. The number of grid points used ranges from 500 to 1400 and was not optimized in each case so that only the first five figures of the total electronic energies are expected to be accurate. However, this accuracy is sufficient for our qualitative analysis.

All calculations are of the Hartree–Fock type, which is appropriate for the identification of the important electronic configuration if other configurations are energetically well separated. This is the case for the systems under consideration here. The calculations have been performed with the fully numerical non-relativistic atomic structure code by Stiehler and Hinze,[35] which was extended for our purposes to include the finite-nucleus potential originating from the hollow, infinitesimally thin sphere [Eq. (2)]:

$$V_{\mathrm{nuc}}(Q,R,r) = \begin{cases} -Q/R \;\; ; \;\; 0 \le r \le R & \text{inside the hollow sphere} \\ -Q/r \;\; ; \;\; r > R & \text{outside the sphere} \end{cases} \tag{2}$$

for the description of the electron-nucleus interaction (R is the radius of the positively charged sphere of thickness zero and Q is the positive charge ($Q = Z$); see reference [36] for a detailed discussion of this and other finite-nucleus potentials). Figure 2 depicts this electron-nucleus interaction potential for two different radii of the positively charged sphere.

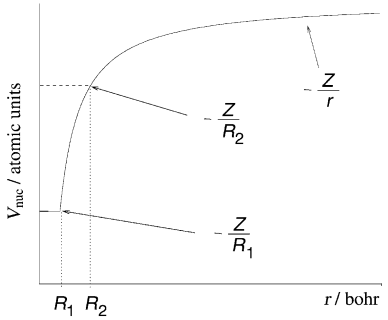

Figure 2. Nuclear potential $V_{nuc}(Q,R,r)$ for two different nucleus sizes R_1 and R_2.

The atomic structure program solves the radial Hartree–Fock equation [Eq. (3)] for a many-electron atom (in Hartree atomic units).[38, 39]

$$\left[-\tfrac{1}{2}\frac{d^2}{dr^2} + \frac{l(l+1)}{2r^2} + V_{nuc}(Z,R,r) + V_{ee}(r,r')\right] P_{nl}(r) = \varepsilon_{nl} P_{nl}(r) \qquad (3)$$

In Equation (3) $V_{ee}(r,r')$ includes all the electron–electron interaction terms and l denotes the angular quantum number. The radial functions $P_{nl}(r)$ are then known on a mesh of grid points. In combination with the angular parts of the atomic orbitals (i.e., the spherical harmonics) the total wave function and the corresponding total electronic energy $\langle E \rangle$ are obtained.

Figure 3 shows the result for an expansion of the nucleus for the rare gas atom krypton ($Z = N = 36$). The atomic orbital energies ε_{nl} are given for each shell in Figure 4. Their correlation between the point-like nucleus case and the expanded nucleus at $R = 2$ bohr is depicted in a Walsh-type diagram.

Since the depth of the potential energy well is small and finite at the end point of the expansion process, the orbitals are spatially extended. Correspondingly, also the energetic order of the orbital energies has changed: ns and np (with $n =$ 2,3,4) are all exchanged upon expansion of the nucleus. The orbitals from the core region are destabilized most, while those from the valence region (4s and 4p in this case) are less affected. This is clear since the highly attractive and singular Coulombic potential has been replaced by a substantially weaker potential. The core orbitals expand largely, but the valence orbitals had their extrema already in the region of $R > 1$ bohr prior to the expansion process.

The new energetic order of the atomic shells of the pseudo-atom is 1s,2p,3d,2s,3p,3s,4s,4p, which is still the electronic ground-state configuration of krypton. Because of the possibility of such changes of the energetic sequence of orbital energies one must be aware of changes in the electronic ground-state configuration. In the latter case, atomic orbitals with different n and l quantum numbers become occupied and

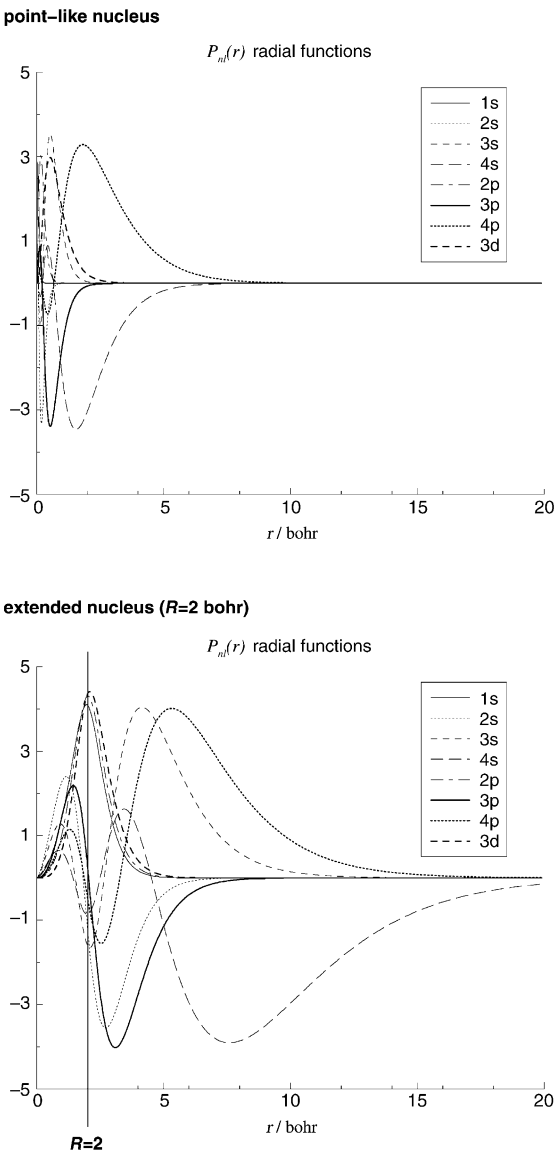

Figure 3. Orbitals for krypton ($Z = N = 36$) with a point-like nucleus (top) and an extended, hollow nucleus with $R = 2$ bohr (bottom).

some from the initial electronic configuration become virtuals. Such additional electronic configurations, which may become the new ground-state configuration, are the more important the more electrons and shells are involved and the closer these shells are in energy. In other words, starting from a given total electronic wave function of a closed-shell atom we may end up with a completely different configuration, that is, a different total wave function with different atomic orbitals. Now, the phenomenological rule found for fullerenes states that the electronic configuration of an aromatic polyhedron at a certain distance R is governed in its valence shell by orbitals with increasing l quantum numbers starting from $l = 0$. This case is not met at the distance R of our example in Figure 4, but might be met at a larger distance, when the 3d orbital is further destabilized and may become the HOMO, while the 3p and 3s orbitals may become the HOMO – 1 and HOMO – 2. However, the "desired" orbital

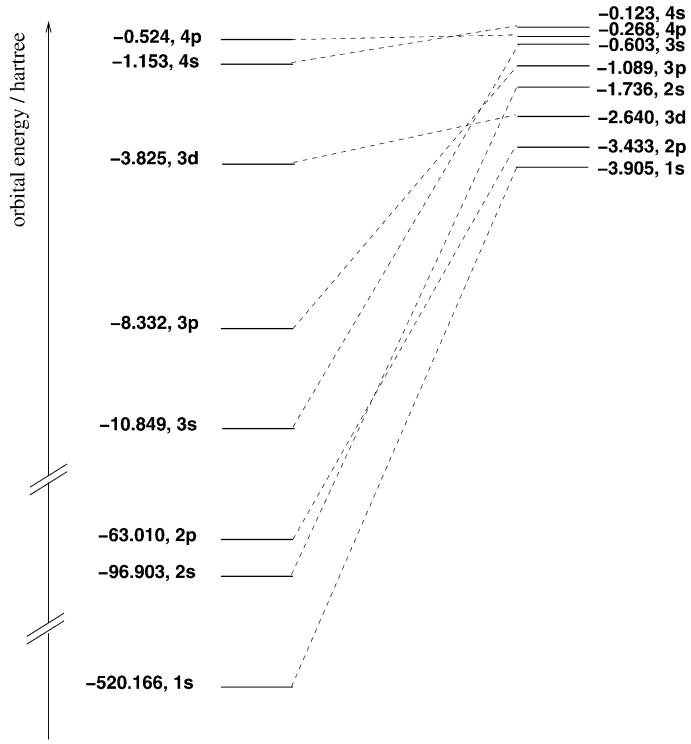

Figure 4. Orbital energies for krypton ($Z=N=36$) with a point-like nucleus (left) and an extended, hollow nucleus with $R=2$ bohr (right).

ordering can also be induced by the radial-symmetry breaking process in phase II.

Of course, for the reconstruction of the $2(N+1)^2$ rule from the point of view of atomic structure, it is necessary to clearly distinguish between pseudo-π and pseudo-σ atomic orbitals.

It should be mentioned at this stage that the correct electronic configuration at the end of phase I can only be safely selected in our single-determinant model if the total electronic energies of these configurations are sufficiently well separated. Otherwise, a multi-configurational formulation, which can be taken into account in our present methodology, and the correct relaxation of the orbitals in phase II, which also changes the orbitals, the orbital energies, and thus the total energy of the pseudo-atom, have to be taken into account.

To conclude from the results for phase I: For a given configuration, that is, for a pre-selected set of occupied atomic orbitals, we calculate the corresponding total electronic energy at any point of the expansion process in phase I. For each of these calculations, the angular part $Y_{lm_l}(\theta,\phi)$ of every orbital remains unchanged and only the radial parts $P_{nl}(r)$ change. This has the important consequence that the angular functions can be classified according to the irreducible representations of the actual point group of the spherical polyhedron in phase II, while the radial functions are responsible for the selection of the ground-state configuration on the basis of the total electronic energy. It is an essential part of the thought experiment that the ground-state configuration for the radial-symmetry-broken polyhedron at the end of phase II need not necessarily be the same as the one for the corresponding atom at the beginning of phase I. The calculations are thus necessary for the selection of the ground-state configuration in the whole process. Once this is achieved, the set of corresponding angular functions $Y_{lm_l}(\theta,\phi)$ is known and can then be subjected to a group-theoretical analysis of the symmetry breaking process. This group-theoretical analysis establishes the connection between the l quantum number classification and the classification according to the irreducible representations of the symmetry-reduced point group of the polyhedron. It is thus the final step in our theoretical approach.

Phase II: In phase II, the spherical symmetry is reduced to, for instance, icosahedral symmetry. This continuous symmetry breaking process can only be described by first-order perturbation theory in the present radial-symmetric formalism, that is, the energy change can only be calculated to first order in the present formulation. However, this might be sufficient for semi-quantitative analyses as has been demonstrated in reference [29].

For such a ligand-field analogous treatment we may define a perturbation operator to the unperturbed Hamiltonian in Equation (4):

$$H^{(1)}=\sum_{i=1}^{N}\frac{-q_i}{R_i}-V_{\mathrm{nuc}}\left(\sum_i q_i,R,r\right) \qquad (4)$$

which describes N positive charges q_i replacing the equal amount of positive charge homogeneously distributed on the sphere with radius $R_i=R$. The amount of charge, $\Sigma_i q_i$, which is condensed at the polyhedron's atomic centers during phase II is subtracted from the original electron–nucleus potential $V_{\mathrm{nuc}}(Z,R,r)$ by $V_{\mathrm{nuc}}(\Sigma_i q_i,R,r)$ entering the perturbation operator. In phase II, the N positive charges q_i are steadily increased until all positive charge is collected at the N atomic centers. This perturbation operator enters secular equations with the spherical harmonics as basis functions selected in phase I. The solutions of these secular equations would yield first-order energy corrections to the original orbital energies. It is evident that this first-order treatment of phase II would be reliable only for systems with many positive charges q_i (i.e., for a many-atom polyhedron), which should be as small as possible. Fullerenes like C_{60} may thus be treated within this approach to phase II, while a molecule like As_4 cannot. In the latter case, the first-order energy corrections would be very large and would thus change all results of phase I, which in turn would destroy the basis of phase II. This could be an indication for the range of validity of the $2(N+1)^2$ rule rather than a demand for a more accurate theoretical approach. But note that even if a system like As_4 cannot appropriately be treated within phase II of the pseudo-atom approach, it can be very well identified as aromatic in terms of magnetic criteria[18] ("aromaticity" cannot solely be judged on an energetical basis; compare the Introduction).

Since the l-classified atomic orbitals in the ground state configuration at the end of phase I split in phase II, we can predict the splitting according to irreducible representations of the actual point group. As basis functions for this group-theoretical analysis we can use the spherical harmonics connected with those radial functions which defined the ground state configuration in phase I. The radial functions are

all totally symmetric so that the symmetry of an atomic orbital is solely governed by the symmetry of the spherical harmonics in a given point group symmetry. For this group-theoretical analysis we have to deduce a reducible representation, which is a collection of characters (traces of the matrices) of the symmetry operations corresponding to the selected set of Y_{lm_l} basis functions (see, e.g., reference [40] for this standard procedure).

Note that the spherical harmonics, which are in use in standard basis functions for the representation of the *molecular* orbitals, are atom-centered in the polyhedra and fullerenes and are thus not to be mixed up with the spherical harmonics in our case, which are centered at the original nucleus' position of the (pseudo-)atom in phase I. Instead, the spherical harmonics, which shall be analyzed here, model exactly those, which were observed phenomenologically in reference [1].

A reduction of the reducible representation obtained for the spherical harmonics basis can be found in standard text books[40] (p. 389). We compare the result of this reduction to irreducible representations of the icosahedral group with the phenomenologically found splitting in reference [1] in Table 1.

Table 1 provides the magic numbers 2, 8, 32, 50, 72, 98, … of π-electrons, which are characteristic for aromaticity in spherical systems. The splitting of molecular orbitals according to irreducible representations of the icosahedral point group given in Table 1 and the stringent requirement of the $2(l_{max}+1)^2$ rule of orbital ordering in spherically symmetric systems also allows us to investigate the range of validity of this rule for fullerenes of increasing size. The larger the fullerenes get the more molecular orbitals are involved in a dense frontier orbital region. At a certain size, when the orbital energies are very close and the splitting in phase II mixes one-electron states, it can be expected that the $2(N+1)^2$ rule approaches its limits. In addition to this analysis of the frontier orbital region according to the symmetry label prediction of Table 1, also the magnetic properties of the large fullerenes can be checked using, for instance, the NICS method.[41]

We should like to add a suggestion for a quantitative method for the symmetry breaking in phase II. Since the atomic structure theory framework, which was essential for the identification of the frontier orbitals and for their l classification, cannot account for the breaking of spherical symmetry, we have to apply molecular electronic structure calculations. These calculations should be designed in such a way that an assignment of molecular orbitals at the beginning of phase II to atomic orbitals at the end of phase I is possible. For this purpose it would be necessary to modify the electron – nucleus interaction integrals in a quantum chemical program package for molecules so that the nuclear charge of all atoms of the molecule is smeared out on the hypothetical sphere defined at the end of phase I. This modification is possible, but not trivial and therefore left for future work.

Table 1. Reduction of the reducible representation spanned by the spherical harmonics basis selected after phase I to irreducible representation of the icosahedral point group I as given in reference [40] (p. 389). The corresponding number of electrons is given in the second column. The total number of electrons follows the $2(l_{max}+1)^2$ rule and is given for each l_{max} row in the third column. The inclusion of the center of inversion yields the additional symmetry labels g and u for gerade and ungerade, respectively. These additional labels can be attached in a straightforward manner according to s,d,g,… orbitals, which are gerade (i.e., l is even), and p,f,h,… orbitals, which are ungerade (i.e., l is odd). They agree with the phenomenological findings in reference [1] (right column).

l	No. e^-	$2(l+1)^2$	I	Ref. [1]
0	2	2	a	a_g
1	6	8	t_1	t_{1u}
2	10	18	h	h_g
3	14	32	t_2+g	$t_{2u}+g_u$
4	18	50	$g+h$	g_g+h_g
5	22	72	t_1+t_2+h	$t_{1u}+t_{2u}+h_u$
6	26	98	$a+t_1+g+h$	
7	30	128	t_1+t_2+g+h	
8	34	162	t_2+g+2h	
9	38	200	$t_1+t_2+2_g+h$	
10	42	242	$a+t_1+t_2+g+2h$	
11	46	288	$2t_1+t_2+g+2h$	
12	50	338	$a+t_1+t_2+2g+2h$	

An Example for an I_h-Symmetric Fullerene: C_{20}^{2+}

For the analysis of the spherically aromatic C_{20}^{2+} we start with the electronic ground-state configuration of Eka-Rn (Uuo). In order to keep the number of protons and electrons the same in our pseudo-atom and in the fullerene we do not analyze Eka-Rn, but the doubly charged Eka-Ra (Ubn) atom, which has the electronic ground-state configuration of Eka-Rn, with 118 electrons and 120 protons. The electronic ground-state configuration for this atomic system can easily be found by applying Madelung's rule. For a continuous expansion of the nuclear charge to an infinitely thin sphere of radius R we should find a change of the ground-state configuration.

The electronic configurations, which are given in Table 2, have been obtained by successively depopulating the core orbitals of the Eka-Rn ground state configuration. There is no a priori recipe for finding the lowest energy configuration. For ordinary atomic structure calculations with point-like atomic nuclei, we can rely on Madelung's rule, which is also only a method that may fail if many electrons are to be distributed over one-electron states. Consequently, we need to find a new recipe that is valid for the hollow sphere distribution of the nuclear charge. Occupation of atomic orbitals with larger angular momentum leads to a decrease in total electronic energy as can be understood from Table 2. However, we observe that this decrease in total electronic energy reaches its maximum at a certain large l value. The *closed-shell* restriction for the atomic configuration, which is imposed by the ground state of the fullerene, has the important consequence that the larger the angular momentum quantum numbers of the atomic orbitals in the configuration are the less closed-shell configurations can be constructed. Note that several other configurations, which are not given in Table 2, have also been tested, but the SCF iterations failed to converge. However, in these cases the SCF iterations oscillated between total

Table 2. Some selected electronic configurations and corresponding total electronic energies (in hartree; Hartree-Fock model) of C_{20}^{2+} for an expanded nucleus of zero thickness with a radius R (in bohr) that approximates the radius of C_{20}^{2+}. For a point-like nucleus ($R=0$), which equals a calculation on Eka-Ra in rare gas configuration of Eka-Rn we would find $[Kr]5s^2,6s^2,7s^2 \mid 5p^6,6p^6,7p^6 \mid 4d^{10},5d^{10},6d^{10} \mid 4f^{14},5f^{14}$ as the ground-state configuration with an electronic energy of -48190.21.

	electronic configuration	$\langle E\rangle(R=4)$
1	$[Kr]5s^2,6s^2,7s^2 \mid 5p^6,6p^6,7p^6 \mid 4d^{10},5d^{10},6d^{10} \mid 4f^{14},5f^{14}$	– 1534.25
2	$[Kr]5s^2 \mid 5p^6,6p^6 \mid 4d^{10},5d^{10},6d^{10},7d^{10} \mid 4f^{14},5f^{14}$	– 1535.33
3	$[Kr]5s^2,6s^2,7s^2,8s^2,9s^2 \mid 5p^6,6p^6,7p^6,8p^6 \mid 4d^{10},5d^{10} \mid 4f^{14},5f^{14}$	– 1526.15
4	$[Kr]5s^2 \mid 5p^6,6p^6,7p^6 \mid 4d^{10},5d^{10} \mid 4f^{14},5f^{14},6f^{14}$	– 1542.56
5	$[Ar]4p^6,5p^6,6p^6 \mid 3d^{10},4d^{10},5d^{10},6d^{10} \mid 4f^{14},5f^{14},6f^{14}$	– 1544.20
6	$[He]2p^6,3p^6,4p^6,5p^6 \mid 3d^{10},4d^{10},5d^{10},6d^{10},7d^{10} \mid 4f^{14},5f^{14},6f^{14}$	– 1535.84
7	$[Kr]5s^2 \mid 4d^{10},5d^{10} \mid 4f^{14},5f^{14},6f^{14} \mid 5g^{18}$	– 1595.87
8	$[Kr]5p^6,6p^6 \mid 4d^{10} \mid 4f^{14},5f^{14},6f^{14} \mid 5g^{18}$	– 1590.81
9	$[Kr]5s^2,6s^2 \mid 5p^6,6p^6 \mid 4d^{10},5d^{10} \mid 4f^{14},5f^{14} \mid 5g^{18}$	– 1591.74
10	$[Kr]5p^6 \mid 4d^{10},5d^{10},6d^{10} \mid 4f^{14},5f^{14} \mid 5g^{18}$	– 1593.22
11	$[Ar]4p^6 \mid 3d^{10},4d^{10},5d^{10} \mid 4f^{14},5f^{14} \mid 5g^{18},6g^{18}$	– 1604.42
12	$2p^6,3p^6,4p^6,5p^6 \mid 3d^{10},4d^{10},5d^{10} \mid 4f^{14},5f^{14} \mid 5g^{18},6g^{18}$	– 1593.60
13	$[He]2p^6,3p^6 \mid 3d^{10},4d^{10},5d^{10},6d^{10} \mid 4f^{14},5f^{14} \mid 5g^{18},6g^{18}$	– 1596.25
14	$3d^{10},4d^{10},5d^{10},6d^{10} \mid 4f^{14},5f^{14},6f^{14} \mid 5g^{18},6g^{18}$	– 1562.05
15	$[Ne]3d^{10},4d^{10},5d^{10} \mid 4f^{14},5f^{14},6f^{14} \mid 5g^{18},6g^{18}$	– 1593.10
16	$[Ar]4s^2 \mid 3d^{10},4d^{10},5d^{10} \mid 4f^{14},5f^{14} \mid 5g^{18} \mid 6h^{22}$	– 1633.47
17	$[Ar]4p^6 \mid 3d^{10},4d^{10},5d^{10},6d^{10} \mid 4f^{14} \mid 5g^{18} \mid 6h^{22}$	– 1619.62
18	$[Ar]3d^{10},4d^{10} \mid 4f^{14} \mid 5g^{18} \mid 6h^{22} \mid 7i^{26}$	**– 1651.69**
19	$[Ar]4s^2,5s^2 \mid 3d^{10},4d^{10} \mid 4f^{14} \mid 5g^{18},6g^{18} \mid 7i^{26}$	– 1622.71
20	$[Kr]4d^{10},5d^{10} \mid 4f^{14} \mid 6h^{22} \mid 7i^{26}$	– 1621.16
21	$[Ne]3s^2 \mid 3d^{10} \mid 5g^{18} \mid 6h^{22} \mid 7i^{26} \mid 8k^{30}$	– 1623.92
22	$[He]2p^6,3p^6 \mid 3d^{10},4d^{10} \mid 4f^{14} \mid 5g^{18} \mid 6h^{22} \mid 8k^{30}$	– 1636.29
23	$[Ne]3p^6 \mid 3d^{10} \mid 4f^{14} \mid 6h^{22} \mid 7i^{26} \mid 8k^{30}$	– 1624.84
24	$[Ne]3d^{10},4d^{10} \mid 4f^{14} \mid 5g^{18} \mid 7i^{26} \mid 8k^{30}$	– 1627.10

electronic energies, which are much higher in energy than the lowest lying configurations given in Table 2.

From Table 2 we understand that the core orbitals in the regular atomic structure calculation with a point-like nucleus are depopulated upon expansion of the nucleus in phase I. The reason for this is that orbitals with large values of l possess similar orbital energies to those with small values of l, so that those orbitals with large values of l, which can take up more electrons the larger their l value is (namely $4l+2$), are energetically favored. However, depopulating all core orbitals with small l values does not lead to even lower energies. From this observation we might deduce the empirical rule that we find a low-energy configuration by distributing a given number of N electrons first on all lowest energy orbitals of different l symmetry (i.e., in the order 1s,2p,3d,4f,5g,6h,7i, …). Then, a number of electrons N_{rest} will remain, since they cannot fill up the $l_{\mathrm{max}}+1$ shell completely. These electrons are then distributed in the same manner starting with the next orbitals in each l symmetry (i.e., 2s,3p,4d,5f,…). This protocol is repeated until all electrons have been distributed. Note that this pocedure obeys the boundary condition that the polyhedron to be modeled is always a closed-shell case, that is, only those atomic configurations need to be tested that are also closed-shell. This observation is in accordance with occupation of orbitals in jellium-type models and, therefore, also with results from the jellium-model treatment of C_{60} in reference [2], in which all shells were classified by the radial quantum number n_r, which counts the number of radial nodes, and by the angular quantum number l. The first series, that is, 1s,2p,3d,4f,5g,6h,7i,…, corresponds to $n_r=0$ since the number of radial nodes is given by $n-l-1$. However, it is common to introduce a new principal quantum number n', which is the number of radial nodes n_r plus one. Our new construction rule for pseudo-atoms is thus 1s,1p,1d,1f,1g,1h,1i,…, until the remaining number of electrons is smaller than the number needed for the next $1\,l_{\mathrm{max}+1}$ shell. Then, we start filling up the next shells (n',l) with one radial node, 2s,2p,2d,2f,… .

The consequence of populating high l orbitals is that only a very small number of orbitals enters the total electronic wave function, since the uptake of electrons by high l orbitals is very large. This is one reason why it was possible to discover the $2(N+1)^2$ rule. It is most striking that one single configuration can be identified from Table 2 (entry 18); this has the lowest energy and is well separated from all other configurations. Most remarkable is the fact that the frontier region is governed by only three s, p, d orbitals, as the $2(l+1)^2$ rule would predict. However, their energetical order is not $\varepsilon_{3s} < \varepsilon_{3p} < \varepsilon_{4d}$, but $\varepsilon_{3p} < \varepsilon_{3s} < \varepsilon_{4d}$ though their orbital energy differences are quite small. The correct ordering could be induced by the symmetry breaking process in phase II. We will come back to this point at the end of this section.

Apart from these three orbitals there is only one other orbital, namely the 7i orbital, which is also in the frontier orbital region; it is the HOMO – 3. This situation is depicted in Figure 5, which gives all orbitals for the spherical model of C_{20}^{2+}.

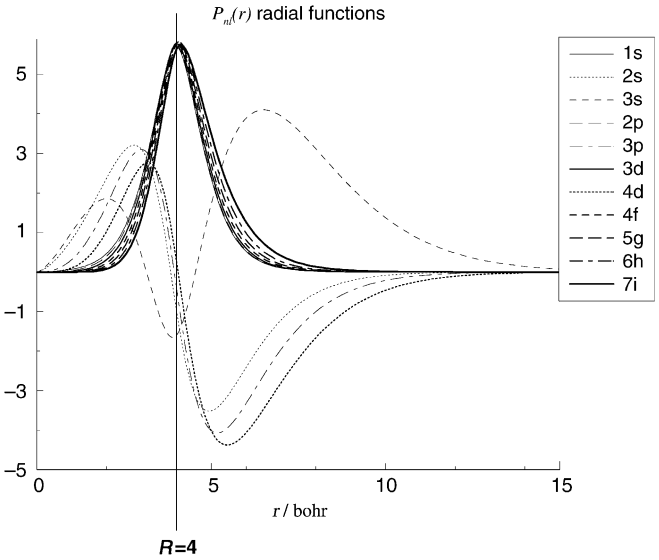

Figure 5. Orbitals for the spherical model of C_{20}^{2+} ($Z=120$, $N=118$) with an extended, hollow nucleus with $R=4$ bohr.

At this stage, we should make some comments on how to distinguish σ- from π-"atomic" orbitals. This question has already been discussed for C_{60} by Martins et al.,[2] who defined all radial-nodeless atomic orbitals as σ-orbitals and those with one (or more) radial node (located exactly at the distance of the hollow sphere's outer shell, i.e., at the position of the positive charge) as a π-orbital. Notice that the HOMO – 3, that is, the 7i (n,l) or 1i (n',l), is a σ-orbital, since it does not have a radial node.

The splitting of the (n',l) frontier atomic orbitals in phase II follows the reduction given in Table 1 for $l = 0,\ldots,2$. We do not provide crystal-field-type calculations for phase II, but instead directly compare with the results at the end of phase II known from molecular Hartree–Fock or density functional calculations (compare, for instance, reference [29] for a crystal-field-type treatment of spherically symmetric one-electron states in C_{60}). In case of C_{20}^{2+} we set up the molecular orbitals from 20 carbon 1s, 20 carbon 2s and certain carbon p atomic orbitals in qualitative MO theory. Therefore, we find 40 electrons in 20 molecular orbitals, which are mainly linear combinations of the set of 1*s* atomic orbitals located at the nuclei of the carbon atoms. In the picture of sp^2 hybridization we find 60 electrons in 30 molecular orbitals, which are constructed from these sp^2 hybrides. The remaining 18 electrons occupy valence molecular orbitals built by p atomic orbitals. Therefore, we conveniently divide the total of 118 electrons into three classes. For the 18 valence electrons (class 3), we expect to find exactly one radial node surface, while we expect none for the 40 core electrons in molecular orbitals generated by the 20 nodeless 1s atomic orbitals (class 1). The σ-bonding electrons in class 2 occupy orbitals that may be expected to have *two* radial nodes, since the 2s atomic orbitals of carbon participate. How two radial nodes may arise in this case is depicted in Figure 6.

From this qualitative analysis we can derive an electronic configuration for the pseudo-atom that is optimal from the molecular point of view. This electronic configuration is given in Table 3.

The pairs of vertical lines || in Table 3 divide the configuration into a closed-shell (left-hand side) and an open-shell (right-hand side): the configurations of classes 1 and 2 possess open-shell configurations in this scheme, while the π-system is closed-shell. Since any electronic structure calculation on this system must assume a singlet state, we may redistribute the ten open-shell electrons from class 2 to class 1 in order to fill the 5g shell. We thus arrive at the configuration $1s^2,2s^2,3s^2,2p^6,3p^6,4p^6,3d^{10},4d^{10},5d^{10},4f^{14},6f^{14},5g^{18},7g^{18}$ for our pseudo-atom calculation, which yields a total electronic energy of -1581.18 hartree. This is considerably smaller in absolute value than our minimum configuration (Table 2; entry 18). The reason is found in the structure of the electronic configuration, which is essentially an excited state, since holes exist in two *l* symmetry series: namely, the 5f and 6g orbitals are unoccupied, while 6f and 7g are not. The corresponding ground-state configuration is entry 11 in Table 2. These ambiguities arise from the oversimplifying requirement of two-radial nodes for the hybrid molecular orbitals of class 2. In contrast with class 1 molecular orbitals, which do not contain any radial node, and class 3 molecular orbitals, which are set up by p-type atomic orbitals that possess a spherical nodal plane that exactly coincides with the carbon-nuclei-carrying sphere, the situation is different for class 2, since the radial symmetry is broken (every 2s orbital possesses a nodal sphere about its carbon nucleus) and the 2s and 2p atomic orbitals hybridize. Therefore, these class 2 orbitals cannot be mapped onto the atomic surrogate orbitals of the pseudo-atom. The radial node discussion partially breaks down for class 2 molecular orbitals.

Table 3. An electronic configuration for the pseudo-atom of C_{20}^{2+} that is optimal from the molecular point of view.

Class	No. e^-	No. radial nodes	n'	(n,l) Configuration
1	40	0	1	$1s^2,2p^6,3d^{10},4f^{14}\,\|\|\,5g^8$
2	60	′2′	3	$3s^2,4p^6,5d^{10},6f^{14},7g^{18}\,\|\|\,8h^{10}$
3	18	1	2	$2s^2,3p^6,4d^{10}\,\|\|$

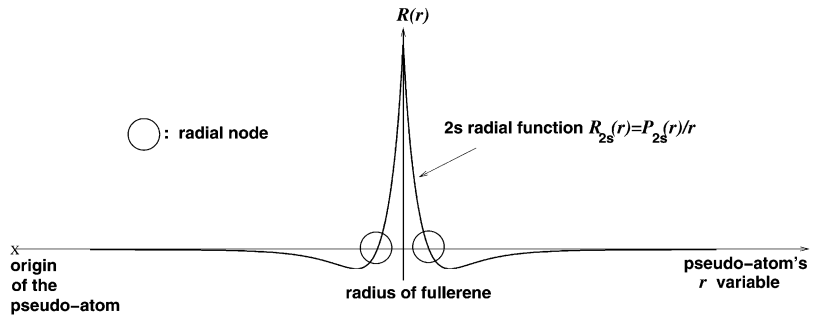

Figure 6. Molecular orbitals constructed by linear combination of 2*s* atomic carbon orbitals would possess two radial nodes in the coordinate frame of the pseudo-atom.

However, these irregularities are artificial and originate from the forced radial symmetry of the pseudo-atom. They arose from the assumption of a certain number of radial nodes for the three classes of molecular orbitals, which is only justified for classes 1 and 3. Nodes in molecular orbitals of class 1 can only arise by negative linear combination of the 1s atomic orbitals centered at the carbon atom's nuclei. In this case the spherical harmonics of the pseudo-atom orbitals account for such nodal structures. After this discussion we arrive at a more stringent definition of a π-orbital in a pseudo-atom or jellium approach: a π-type (pseudo) atomic orbital possesses exactly one radial node. Notice that this definition differs from that in reference [2], in which all orbitals with one *or more* radial nodes are called π-type orbitals.

Now we understand that the previously found orbital ordering of 3p,3s,4d will be changed largely in phase II, since the correct s-orbital to be found for the π-sytem must possess only one radial node; this must, therefore, be a 2s orbital. The 2s orbital in the configuration given in entry 18 in Table 2 is the HOMO – 4. Consequently, we find the following orbital ordering for the π-system: 2s(HOMO-4), 3p(HOMO-2), 4d(HOMO). The orbital ordering thus exactly fulfills the $2(N+1)^2$ rule, though these π-orbitals are interfered with by intruder orbitals, which will significantly be lowered in energy upon charge condensation during phase II. This lowering of orbital energies can be understood from Figure 3, in which the effect is demonstrated for krypton. In the case of a fullerene, the shift of *atomic* orbital energy levels occurs for every carbon atom of the fullerene sphere when the nuclear charge is contracted or expanded as it is done in phase II.

To conclude from these observations, it is possible to identify the π-orbitals on the basis

of the requirement that they must be represented by (pseudo-)atomic orbitals with exactly one radial node. In the case of C_{20}^{2+} we obtain the correct orbital ordering of the π-sytem already after phase I, though there is interference by orbitals that become lower in energy only at the end of phase II.

Conclusions and Perspective

In the present work we have demonstrated how the $2(N+1)^2$ rule of spherical aromaticity can be understood from the point of view of atomic structure theory. Apart from the heuristic value of this viewpoint, it might gain practical value if its predictive power is investigated in greater detail. For this purpose it is necessary for future studies to analyze the following questions:

1) Is it possible in all cases of aromatic polyhedra to clearly select a single ground-state configuration that is significantly well separated from alternative configurations?
2) Is it possible to predict which symmetry breaking procedure is favored if the positive charge can be contracted in various ways so that atomic nuclei of different atoms are generated (at various positions) on the surface of the sphere in phase II?

The first point could be checked for various aromatic polyhedra within the presented methodology. Furthermore, the inverse check can be omitted, since it was found for non- or weakly aromatic fullerenes like C_{20} that the valence shells are only partially occupied; this easily leads to multi-configurational cases so that no unique single configuration can be selected. However, it might be possible to predict point-group symmetry reductions, which are, for example, observed for the neutral systems C_{20} and C_{60}, by using crystal-field techniques along the lines of Jahn–Teller distortions. The accuracy of our single-determinantal Hartree–Fock model could be improved by a DFT model, which is capable of treating dynamic electron correlation effects. However, we did not find a hint that this would be of decisive importance for this study.

Most decisive for the $2(N+1)^2$ rule is a clear-cut definition of its range of applicability. Though this rule was confirmed by NICS studies, we so far relied only on energy criteria, which attribute a pronounced stability, that is, a low total electronic energy, to those clusters that obey the rule. Within our energy analysis we gave boundary conditions that should be fulfilled for a meaningful application of the rule. In turn, phase II of the pseudo-atom description defines also the limits of jellium-type approaches to the description of spherical fullerenes. As we demonstrated at the end of the last section, it is particularly the σ-bonded valence electron system that cannot appropriately be mapped onto the spherically symmetric atomic orbitals of the pseudo-atom.

While phase I is evidently possible for any kind of spherical, hollow cluster or fullerene, the change of one-electron states in phase II can be dramatic. Imagine, for instance, a cluster with total proton charge of +180 that is contracted in phase II at six positions of an octahedron. This contraction will change the electronic structure significantly and a perturbative treatment is not possible. The selected configuration at the end of phase I is thus no longer the parent configuration for the one-electron states that emerge at the end of phase II in such a case in which the contraction of the positive charges at certain points is no longer a small perturbation. On the basis of this qualitative reasoning we could extract an energy measure for the breakdown of the $2(N+1)^2$ rule. Such a measure could be related to the splitting of a given l-shell (n',l). In case of large splittings, the molecular orbitals of different (n',l)-shells may strongly interact and mix so that the frontier orbital region cannot be interpreted. Fortunately, it is not necessary to carry out this analysis within the approximations of a crystal-field-type framework; it can be done by comparison with the molecular orbitals obtained from molecular calculations, as has been demonstrated above for C_{20}^{2+}.

Another implication of our energy criterion becomes evident in the following. According to the $2(N+1)^2$ rule, the π-electron system of C_{60}^{10+} is aromatic, while the one in C_{60} is not. How can this be understood in our pseudo-atom model? In a molecular orbital calculation, both fullerenes are closed-shell, singlet molecules. Within our pseudo-atom model, however, this is no longer the case. While C_{60}^{10+} possesses a closed l_{max}-shell, the ten additional electrons of C_{60} are "filled" in the next l_{max+1}-shell, which is then an open-shell at the end of phase I. The charge contraction in phase II will lower the symmetry such that the l_{max+1}-shell splits and the sub-shell is completely filled. However, if the perturbation introduced by phase II on the electronic configuration of phase I is not too large, the energy splitting of the l_{max+1}-shell will be small. This implies that the HOMO–LUMO gap in a molecular orbital theory, which provides occupation-number-independent one-electron states (like the extended Hückel method does), should be small. The electronic ground-state wave function of C_{60} should thus be more multi-configurational in nature than the one of C_{60}^{10+}.

We have demonstrated that our pseudo-atom approach is useful for understanding the special features of one-electron states in fullerenes. The discussion has revealed some interesting questions for testing the range of validity of the $2(N+1)^2$ rule for spherical aromaticity, which should be tackled in future work.

Acknowledgements

Financial support from the Collaborative Research Center SFB 583 and from the Fonds der chemischen Industrie is gratefully acknowledged.

[1] A. Hirsch, Z. Chen, H. Jiao, *Angew. Chem.* **2000**, *112*, 4079–4081; *Angew. Chem. Int. Ed.* **2000**, *39*, 3915–3917.
[2] J. L. Martins, N. Troullier, J. H. Weaver, *Chem. Phys. Lett.* **1991**, *180*, 457–460.
[3] E. D. Jemmis, P. von R. Schleyer, *J. Am. Chem. Soc.* **1982**, *104*, 4781–4788.
[4] R. C. Haddon, *Acc. Chem. Res.* **1988**, *21*, 243–249.
[5] M. Deza, P. W. Fowler, A. Rassat, K. M. Rogers, *J. Chem. Inf. Comput. Sci.* **2000**, *40*, 550–558.
[6] R. B. King, *Chem. Phys. Lett.* **2001**, *338*, 237–240.
[7] R. B. King, *Chem. Rev.* **2001**, *101*, 1119–1152.
[8] R. B. King, *J. Math. Chem.* **1998**, *23*, 197–227.
[9] "Topological Aspects of Carbon Allotrope Structures": R. B. King, *Math. Chem.* **1999**, *5*, 85–128.
[10] G. J. Miller, J. G. Verkade, *J. Math. Chem.* **2003**, *33*, 55–79.

[11] P. W. Fowler, G. Caporossi, P. Hansen, *J. Phys. Chem. A* **2001**, *105*, 6232 – 6242.
[12] A. J. Stone. *Mol. Phys.* **1980**, *41*, 1339 – 1354.
[13] A. J. Stone. *Inorg. Chem.* **1981**, *20*, 563 – 571.
[14] Z. Chen, H. Jiao, A. Hirsch, W. Thiel, *J. Mol. Model.* **2001**, *7*, 161 – 163.
[15] Z. Chen, J. Cioslowski, N. Rao, D. Moncrieff, M. Bühl, A. Hirsch, W. Thiel, *Theor. Chem. Acc.* **2001**, *106*, 364 – 368.
[16] Z. Chen, H. Jiao, M. Bühl, A. Hirsch, W. Thiel, *Theor. Chem. Acc.* **2001**, *106*, 352 – 363.
[17] M. Bühl, A. Hirsch, *Chem. Rev.* **2001**, *101*, 1153 – 1183.
[18] A. Hirsch, Z. Chen, H. Jiao, *Angew. Chem.* **2001**, *113*, 2916 – 2920; *Angew. Chem. Int. Ed.* **2001**, *40*, 2834 – 2838.
[19] Z. Chen, H. Jiao, A. Hirsch, P. von R. Schleyer, *Angew. Chem.* **2002**, *114*, 4485 – 4488; *Angew. Chem. Int. Ed.* **2002**, *41*, 4309 – 4312.
[20] A. R. Katritzky, P. Barczynski, G. Musumarra, D. Pisano, M. Szafran, *J. Am. Chem. Soc.* **1989**, *111*, 7 – 15.
[21] A. R. Katritzky, M. Karelson, N. Malhorta, *Heterocycles* **1991**, *32*, 127 – 161.
[22] K. Jug, A. M. Köster, *J. Phys. Org. Chem.* **1991**, *4*, 163 – 169.
[23] T. M. Krygowski, A. Ciesielski, C. W. Bird, A. Kotschy, *J. Chem. Inf. Comput. Sci.* **1995**, *35*, 203 – 210.
[24] "Aromatizität—Geschichte und mathematische Analyse eines fundamentalen chemischen Begriffs": J. Neus, *HYLE Studies in History and Philosophy of Chemistry, Vol. 2*, HYLE Publications Karlsruhe, www.hyle.org/publications **2002**.
[25] M. R. Manaa, D. W. Sprehn, H. A. Ichord, *J. Am. Chem. Soc.* **2002**, *124*, 13990 – 13991.
[26] D. Andrae, M. Reiher, J. Hinze, *Chem. Phys. Lett.* **2000**, *320*, 457 – 468.
[27] C. Kittel, *Quantum Theory of Solids*, 2nd ed., Wiley, New York, **1987**.
[28] "Introduction to Solid-State Theory": O. Madelung, *Springer Ser. Solid-State Sci*. **1978**, *2*, whole volume.
[29] C. Yannouleas, U. Landman, *Chem. Phys. Lett.* **1994**, *217*, 175 – 185.
[30] D. Bauer, F. Ceccherini, A. Macchi, F. Cornolti, *Phys. Rev. A* **2001**, *64*, 063203.
[31] D. M. P. Mingos, Z. Lin, *Chem. Phys.* **1989**, *137*, 15 – 24.
[32] A. J. Stone, M. J. Alderton, *Inorg. Chem.* **1982**, *21*, 2297 – 2302.
[33] A. J. Stone, *Polyhedron* **1984**, *3*, 1299 – 1306.
[34] T. R. Walsh, D. J. Wales, *J. Chem. Phys.* **1998**, *109*, 6691 – 6700.
[35] "Der numerische Multiconfiguration-Self-Consistent-Field-Ansatz für Atome": J. Stiehler, Ph.D. Thesis, Universität Bielefeld, **1995**.
[36] D. Andrae, *Phys. Rep.* **2000**, *336*, 413 – 525.
[37] D. R. Hartree, *The Calculation of Atomic Structures*, Wiley, New York, **1957**.
[38] C. Froese Fischer, *The Hartree – Fock Method for Atoms*, Wiley, New York, **1977**.
[39] L. Szasz, *The Electronic Structure of Atoms*, Wiley, New York, **1992**.
[40] J. S. Griffith, *The Theory of Transition-Metal Ions*, Cambridge University Press, Cambridge, **1964**.
[41] P. von R. Schleyer, C. Maerker, A. Dransfeld, H. Jiao, N. J. R. van E. Hommes, *J. Am. Chem. Soc.* **1996**, *118*, 6317 – 6318.